Niche engineering demonstrates a latent capacity for fungal-algal mutualism

Erik F. Y. Hom and Andrew W. Murray

Science **345**, 94 (2014);
DOI: 10.1126/science.1253320

Science (print ISSN 0036-8075; online ISSN 1095-9203) is published weekly, except the last week in December, by the American Association for the Advancement of Science, 1200 New York Avenue NW, Washington, DC 20005.

Text

basement membrane at P0 (fig. S11, B and C). However, at P7, endocardial cells and their derivatives (labeled by Tie2-Cre or VE Cad-CreER) were no longer aligned with COL3A1 strands but rather took up intramyocardial positions (P7 in fig. S11, B and C). To better visualize the process by which P0 endocardium transforms into intramyocardial VECs at P7, we studied an intermediary stage (P3) when hearts contain both unremodeled trabeculae (Fig. 4B) and actively compacting regions (Fig. 4C). We labeled developmental intermediates by treating Apln-CreER; Rosa26$^{mTmG/+}$ mice with tamoxifen at P1.5 (Fig. 4A). Trapped endothelial cells remote from the basement membrane adopted the morphology of individual capillary-like cells and were marked by the VEC genetic lineage tracer (green fluorescent protein, see GFP in Fig. 4C), whereas endothelial cells facing the ventricular lumen and residing on the basement membrane retained sheetlike morphology and did not express VEC lineage tracer, consistent with endocardial identity (Fig. 4B). These observations suggest that myocardial compaction traps sheets of endocardial cells, which convert to the VEC lineage and translocate to an intramyocardial location.

We investigated conditions that might promote endocardium to VEC transition in the neonatal heart. Hypoxyprobe, a hypoxia-sensitive chemical probe, indicated that rapid expansion of the compact myocardium by trabecular coalescence in the first several postnatal days of life creates a hypoxic environment within the inner myocardial wall (fig. S12). Expression of hypoxia inducible factor 1α (*Hif1α*) and vascular endothelial growth factor A *Vegfa*, genes known to be up-regulated by hypoxia, increased in the inner myocardial wall of the P1 and P3 neonatal hearts (fig. S12, B and C). This corresponds to the region in which we observed endocardial to VEC lineage conversion, suggesting that hypoxia and its resulting up-regulation of the key angiogenic factor Vegfa contribute to this process.

Our work reveals a mechanism by which trabecular coalescence and endocardial-to-VEC lineage conversion drive vascular expansion in the postnatal heart. Why does coronary vascular growth in this setting rely on this alternative mechanism, rather than occurring through more typical angiogenic sprouting from preexisting vessels? The transition from fetal to postnatal circulation acutely increases the hemodynamic burden on the left ventricle. To accommodate this increased workload, we reason that mammals developed trabecular myocardium as a reservoir of new cardiomyocytes that is quickly recruited after birth through myocardial compaction to increase neonatal left ventricular mass. In addition to cardiomyocytes, this myocardial reservoir also contains coronary vessel precursors in the form of endocardial cells. Trabeculae coalesce during neonatal myocardial compaction causes regional hypoxia that stimulates the trapped neonatal endocardial cells to form the vascular supply for the newly compacted myocardium. This mechanism likely allows more rapid vascular and myocardial growth than angiogenic sprouting of the first CVP from the periphery. Understanding this endogenous mechanism for rapidly developing a functional vascular supply has important implications for cardiac diseases and cardiac regenerative medicine (*4*).

REFERENCES AND NOTES

1. P. R. Riley, N. Smart, *Cardiovasc. Res.* **91**, 260–268 (2011).
2. B. A. Yi, O. Wernet, K. R. Chien, *J. Clin. Invest.* **120**, 20–28 (2010).
3. N. Smart *et al.*, *Nature* **445**, 177–182 (2007).
4. E. R. Porrello *et al.*, *Science* **331**, 1078–1080 (2011).
5. H. S. Bennett, *Am. J. Anat.* **60**, 27–53 (1936).
6. K. Red-Horse, H. Ueno, I. L. Weissman, M. A. Krasnow, *Nature* **464**, 549–553 (2010).
7. T. C. Katz *et al.*, *Dev. Cell* **22**, 639–650 (2012).
8. B. Wu *et al.*, *Cell* **151**, 1083–1096 (2012).
9. P. Riley, *Nature* **464**, 498–499 (2010).
10. G. del Monte, P. Richard, *Cell* **151**, 932 (2012).
11. X. Tian *et al.*, *Cell Res.* **23**, 1075–1090 (2013).
12. D. Sedmera, T. Pexieder, M. Vuillemin, R. P. Thompson, R. H. Anderson, *Anat. Rec.* **258**, 319–337 (2000).
13. H. Elmasri *et al.*, *FASEB J.* **23**, 3865–3873 (2009).
14. B. Zhou *et al.*, *Development* **132**, 1137–1146 (2005).

ACKNOWLEDGMENTS

We thank K. Red-Horse, Y. Chen, and N. Jin for insightful discussions and R. Adams, H. Zeng, Z. Yang, T. Quertermous, J. Rossant, and A. Nagy for mouse strains. This work was supported by National Basic Research Program of China (2012CB945102 and 2013CB945302), National Natural Science Foundation of China (91339104, 31271552, 31222038, 31301188), Chinese Academy of Sciences (Hundred Talents Program and KSCX2-EW-R-09), Shanghai Pujiang Program (11PJ1411400) and Basic Research Key Project (14JC1407400), Organization Department of the CPC Central Committee Bajian Talents Program, AstraZeneca, Sanofi-Aventis Shanghai Institutes for Biological Sciences (SA-SIBS) Fellowship, Postdoc Fund (SIBS-2013KIP311, China-2013M541561), NIH (2 R01 HL094683), and American Heart Association Established Investigator Award to W.T.P.

SUPPLEMENTARY MATERIALS

www.sciencemag.org/content/345/6192/90/suppl/DC1
Materials and Methods
Figs. S1 to S12
References (*15*–*25*)

29 January 2014; accepted 22 May 2014
10.1126/science.1251487

PLANT-FUNGAL ECOLOGY

Niche engineering demonstrates a latent capacity for fungal-algal mutualism

Erik F. Y. Hom[1,2]*† and Andrew W. Murray[1,2]*

Mutualistic symbioses shape the evolution of species and ecosystems and catalyze the emergence of biological complexity, yet how such symbioses first form is unclear. We show that an obligate mutualism between the yeast *Saccharomyces cerevisiae* and the alga *Chlamydomonas reinhardtii*—two model eukaryotes with very different life histories—can arise spontaneously in an environment requiring reciprocal carbon and nitrogen exchange. This capacity for mutualism is phylogenetically broad, extending to other *Chlamydomonas* and fungal species. Furthermore, we witnessed the spontaneous association of *Chlamydomonas* algal cells physically interacting with filamentous fungi. These observations demonstrate that under specific conditions, environmental change induces free-living species to become obligate mutualists and establishes a set of experimentally tractable, phylogenetically related, synthetic systems for studying the evolution of symbiosis.

Mutualistic symbioses—beneficial associations between different species involving persistent physical contact and physiological coupling—are central to many evolutionary and ecological innovations (*1*–*3*). These include the origin of eukaryotic cells, the colonization of land by plants, coral reefs, and the gut microbiota of insects and animals (*4*, *5*). Despite their ubiquity and importance, we understand little about how mutualistic symbioses form between previously free-living organisms (*5*, *6*). Like speciation, the birth of novel symbioses has rarely been witnessed, making it difficult to determine if coevolution occurs before symbiosis begins or if chance ecological encounters initiate new symbioses (*5*, *7*). Such "ecological fitting" (*8*, *9*) occurs when both a particular environment and previously evolved traits allow a set of species to complement each other, giving rise to novel interactions without the need for prior coevolutionary adaptation.

We tested two genetically tractable organisms, the budding yeast *Saccharomyces cerevisiae* and the green alga *Chlamydomonas reinhardtii*, to determine if a reciprocal exchange of carbon and nitrogen would lead to obligate mutualism between algae and fungi such as those that occur naturally (*10*–*13*). In our scheme (Fig. 1A), *S. cerevisiae* metabolizes glucose to carbon dioxide (CO_2), a carbon source that *C. reinhardtii* fixes via photosynthesis, and *C. reinhardtii* reduces nitrite (NO_2^-) into ammonia (NH_3) (*14*), which yeast can use as a nitrogen source. Coculturing

[1]Department of Molecular and Cellular Biology, Harvard University, Cambridge, MA 02138, USA. [2]Faculty of Arts and Sciences Center for Systems Biology, Harvard University, Cambridge, MA 02138, USA.
***Corresponding author. E-mail: erik@fyhom.com; amurray@mcb.harvard.edu** †Present address: Department of Biology, University of Mississippi, University, MS 38677, USA.

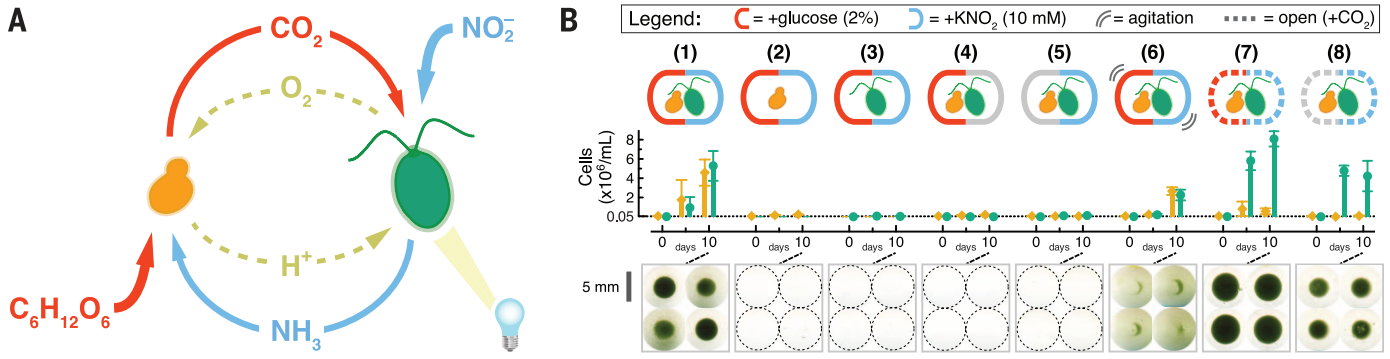

Fig. 1. A synthetic mutualism between *S. cerevisiae* and *C. reinhardtii*. (**A**) A metabolic circuit for mutualism based on carbon and nitrogen exchange. *S. cerevisiae* (orange, left) metabolizes glucose ($C_6H_{12}O_6$) and releases carbon dioxide (CO_2), which is assimilated photosynthetically by *C. reinhardtii* (green, right) to release oxygen (O_2); *C. reinhardtii* metabolizes nitrite (NO_2^-) and releases ammonia (NH_3) as a nitrogen source for *S. cerevisiae*. An intrinsic, near-neutral pH balance between 6.8 and 7.4 is maintained by a metabolic exchange of protons between yeast and alga. (**B**) Proliferation of *S. cerevisiae* and *C. reinhardtii* under different coculture conditions demonstrates that obligate mutualism can arise without any genetic engineering of metabolic pathways. Top: cartoons of the different conditions tested; middle: cell density of yeast and alga over the course of the experiment (mean ± 95% confidence interval; $N = 4$); bottom: images of the cell populations from four representative examples of each culture condition (after 10 days). The dark green hue of the pellets is due to *C. reinhardtii* cells; *S. cerevisiae* cells are off-white and are interspersed throughout the pellet. See (*15*) for further details.

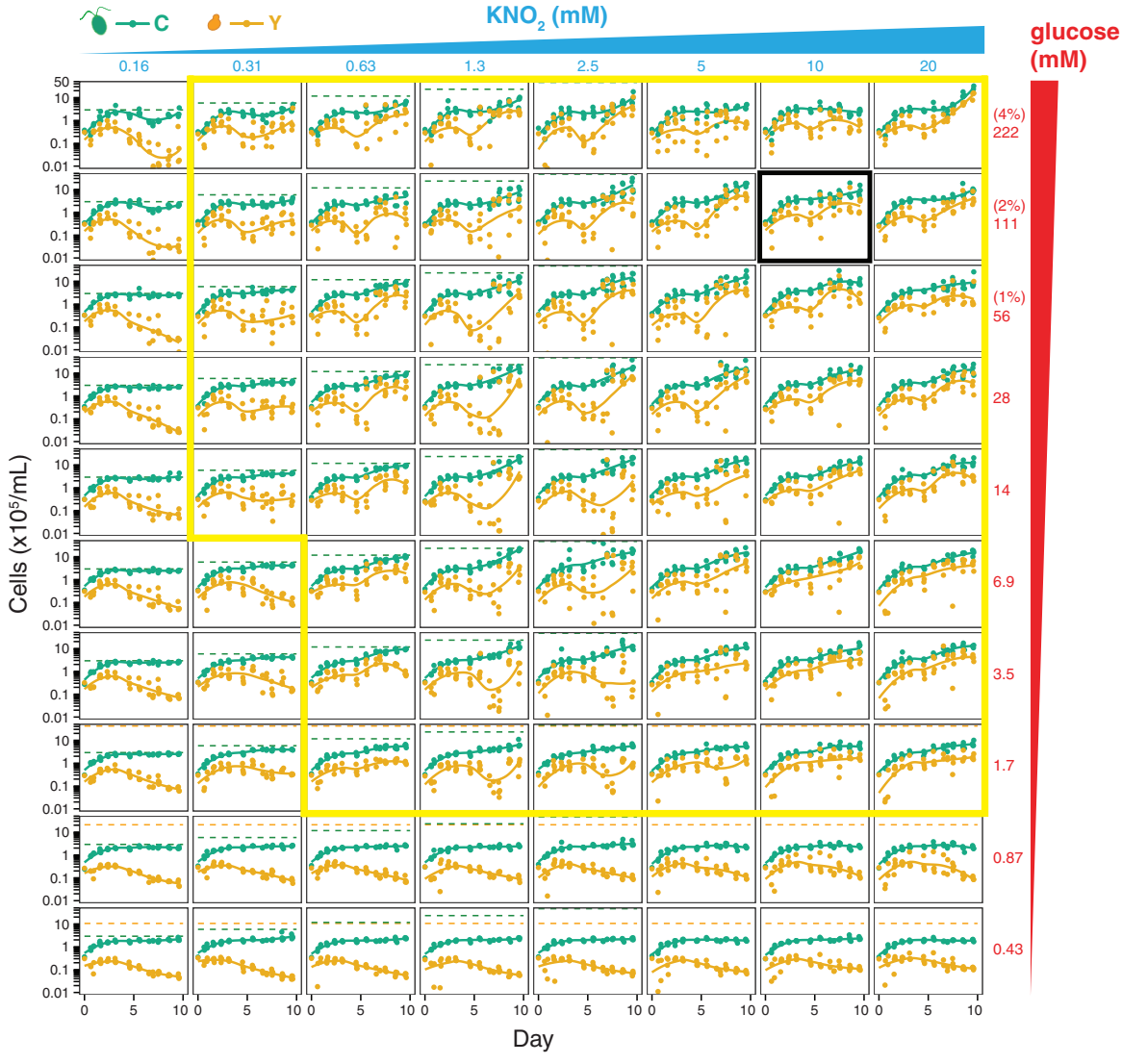

Fig. 2. Landscape of mutualistic productivity. Cell densities over time for each species grown in coculture (*C. reinhardtii* in green; *S. cerevisiae* in orange) grown from an initial inoculum of ~0.3 × 10^5 cells/ml for each species; irradiance = 110 μmol m^{-2} s^{-1}. Each of four replicate point pairs (green and orange) is plotted. Local polynomial regression fits (by robust linear regression in *R* with $y \sim x$) for both cell types are plotted as a visual guide of cell proliferation. Coculture conditions are denoted on the top and right and show increasing (left to right) KNO_2 concentration and increasing (bottom to top) glucose concentration. The standard conditions of 10 mM KNO_2 and 111 mM (2%) glucose used in Fig. 1 are outlined by a black box. Dashed lines indicate the maximum predicted cell densities expected for *C. reinhardtii* (green) and *S. cerevisiae* (orange) for each coculture (*15*). Net positive proliferation of both yeast and algae is supported within the region bounded by the yellow outline. The limited proliferation of *C. reinhardtii* under conditions outside this region (in days 1 and 2) indicates residual atmospheric CO_2 in the wells of the sealed microtiter plate.

experiments (*15*) indicate that by preventing access to atmospheric CO_2, *S. cerevisiae* and *C. reinhardtii* become obligate mutualists (Fig. 1B). This mutualism depends on the metabolic capabilities of the two organisms: *S. cerevisiae* cannot use nitrite as a nitrogen source and *C. reinhardtii* cannot use glucose as a carbon source. Cell proliferation did not require genetic engineering or fine-tuning of nutrient concentrations or starting ratios of the two species (Fig. 1B and figs. S1 and S2) and failed when either species (Fig. 1B, conditions 2 and 3), glucose, or nitrite was omitted from the experiment (Fig. 1B, conditions 4 and 5). Agitation attenuates this mutualism (Fig. 1B, condition 6), suggesting the importance of cell-cell proximity and spatial structure in establishing successful cooperation (*16*). Thus, a simple environmental change can induce free-living organisms to be mutualistic without requiring adaptive coevolution.

In our scheme, mutualism can be obligate or facultative depending on the environment. Access to atmospheric CO_2 makes *C. reinhardtii* a facultative mutualist by removing its dependence on *S. cerevisiae* for carbon (Fig. 1B, condition 7), but the yeast remains dependent on the alga for nitrogen. In this environment, algal proliferation is improved by the presence of glucose-metabolizing, CO_2-generating budding yeast whereas yeast proliferation is reduced, although not extinguished (Fig. 1B, compare conditions 7 and 8). Conversely, adding ammonia (as ammonium chloride) to airtight cocultures allows budding yeast to proliferate independently of the alga whereas the alga remains dependent on the yeast for carbon. Under these conditions, *S. cerevisiae* (~4 hours doubling time in our conditions) outproliferates *C. reinhardtii* (≥12 hours doubling time) and drives the alga to near extinction (fig. S1, condition 15). These results suggest that stable metabolic mutualisms require that the faster-growing species be obligately dependent on nutrients produced by its slower-growing partner.

The engineered obligate mutualism between *S. cerevisiae* and *C. reinhardtii* is not limited to our initial choice of input nutrient concentrations. Successful mutualisms were established over nearly two orders of magnitude in glucose and nitrite concentrations (Fig. 2). However, this resulted in complex population dynamics. We observed undulations and variations in stability across time similar to density-dependent population cycles predicted for mutualistic systems (*17*). Other carbon (e.g., galactose) or nitrogen (e.g., nitrate) sources, although less effective, also sustain mutualism between *S. cerevisiae* and *C. reinhardtii* (fig. S3).

We also demonstrate that many different ascomycetous yeast and four *Chlamydomonas* species, spanning over 300 million years of evolutionary divergence in each clade, can form mutualisms (Fig. 3). Nearly all yeast species we examined form synthetic obligate mutualisms with *C. reinhardtii*, although with different degrees of productivity (Fig. 3A). Mutualistic productivity, as assessed by total cell counts, did not correlate with a yeast's preference for a fermentative or respiratory lifestyle (Fig. 3A), whether a yeast strain was isolated from soil (a potential habitat shared with *C. reinhardtii*), intrinsic growth rate, or nitrite-mediated inhibition of growth (fig. S4 and table S1). Thus, we observe that mutualisms can be phylogenetically broad, but that the degree of success depends on species-specific traits.

Two yeast species and the alga *Chlorella vulgaris* did not form obligate mutualisms (Fig. 3). *C. vulgaris*, which can use glucose as a carbon source, outproliferated *S. cerevisiae*, whereas

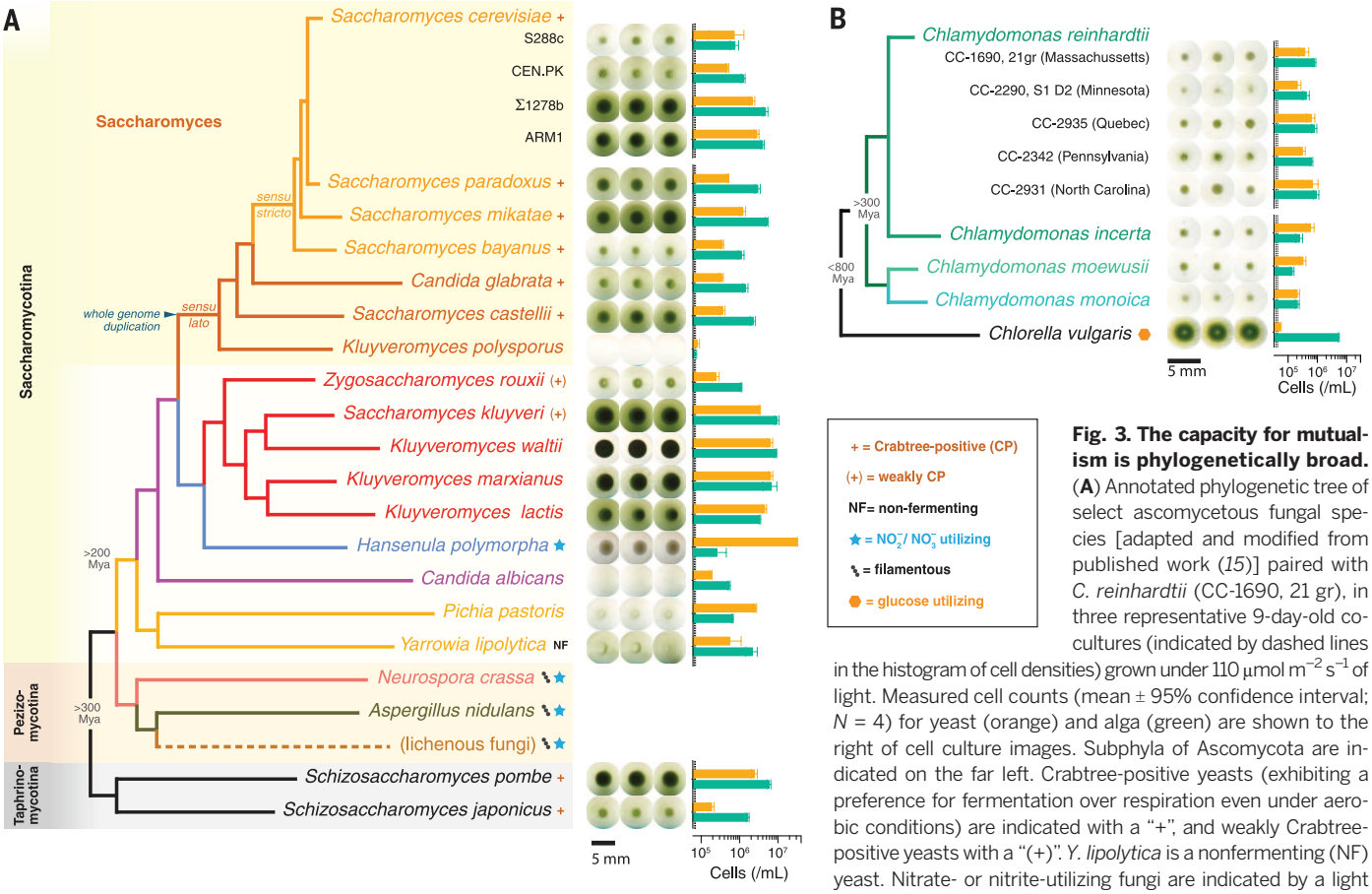

Fig. 3. The capacity for mutualism is phylogenetically broad. (**A**) Annotated phylogenetic tree of select ascomycetous fungal species [adapted and modified from published work (*15*)] paired with *C. reinhardtii* (CC-1690, 21 gr), in three representative 9-day-old cocultures (indicated by dashed lines in the histogram of cell densities) grown under 110 μmol m^{-2} s^{-1} of light. Measured cell counts (mean ± 95% confidence interval; $N = 4$) for yeast (orange) and alga (green) are shown to the right of cell culture images. Subphyla of Ascomycota are indicated on the far left. Crabtree-positive yeasts (exhibiting a preference for fermentation over respiration even under aerobic conditions) are indicated with a "+", and weakly Crabtree-positive yeasts with a "(+)". *Y. lipolytica* is a nonfermenting (NF) yeast. Nitrate- or nitrite-utilizing fungi are indicated by a light blue star and filamentous fungi by three connected dots (see fig. S5). (**B**) Annotated phylogenetic tree [adapted and modified from published work (*15*)] of select algal species and *Chlamydomonas* cultivars (green bars at right) paired with *S. cerevisiae* (S288C) (orange bars, right) in representative 7-day-old cocultures grown under 110 μmol m^{-2} s^{-1} of light (mean ± 95% confidence interval; $N = 12$). *Chlorella vulgaris* is an asexual alga, distantly related to *C. reinhardtii*, and able to use glucose as a carbon source (orange hexagon). Descriptions of strains are provided in table S1.

Hansenula polymorpha, a yeast that can use nitrite as a sole nitrogen source, outproliferated *C. reinhardtii*. The yeast *Kluveromyces polysporus* failed to form an obligate mutualism with *C. reinhardtii*. This yeast can grow in an ammonium-supplemented coculture medium, suggesting that it fails to cooperate with *C. reinhardtii* likely because it either cannot grow at the low ammonia levels produced by *C. reinhardtii* or is more sensitive to nitrite inhibition at such low ammonia levels (fig. S4). *Neurospora crassa* and *Aspergillus nidulans* are genetically tractable filamentous fungi that can use nitrite as a nitrogen source (*18*). The ability of these fungi to reduce nitrite keeps wild-type strains from forming obligate mutualisms with *C. reinhardtii*. However, mutants that cannot reduce nitrite did form obligate mutualisms (fig. S5), suggesting that a loss of gene function in one species could be complemented through mutualism (*7*, *19*).

We observed that the filamentous fungi formed macroscopic structures (fig. S5) such that the fungal hyphae were decorated with *C. reinhardtii* cells (Fig. 4, A and B, and movies S1 to S6). However, physical associations between fungus and alga form even in the absence of any metabolic dependency (figs. S6 and S7 and movies S7 to S16). Electron microscopy of interactions between *C. reinhardtii* and *A. nidulans*, which shares a most recent common ancestor with lichenous fungi within the class Eurotiomycetes (*10*), revealed a tight fungal-algal contact interface (Fig. 4, C and D) reminiscent of wall-to-wall interfaces between fungal and algal cells in extant lichens (*20*). The walls of *C. reinhardtii* cells in contact with *A. nidulans* hyphae are less heavily stained and appear thinner than *C. reinhardtii* cells cultured separately (Fig. 4E), possibly because of locally secreted *A. nidulans* cell wall–remodeling enzymes. We saw no evidence of any morphologically complex tissue structures, such as those seen in many lichens, nor of fungal hyphae penetrating algal cells (*11*, *20*). Thus, these synthetic mutualisms may result in physical complexes but they do not appear to form elaborate morphological structures at the cellular or organismal level.

The ease with which fungal-algal mutualisms were created suggests that ecological interactions may be relatively easy to establish (*21*). Furthermore, they do not require a prior facultative, commensal, or parasitic stage, or coevolutionary adaptation (*5*–*7*, *22*, *23*). Our understanding of how "ecologically framed" pairs of species can be created in response to environments that force them to depend on each other will be useful in the emerging field of synthetic ecology (*24*, *25*), as well as for understanding the assembly of microbial communities in cases of disturbed or invaded habitats.

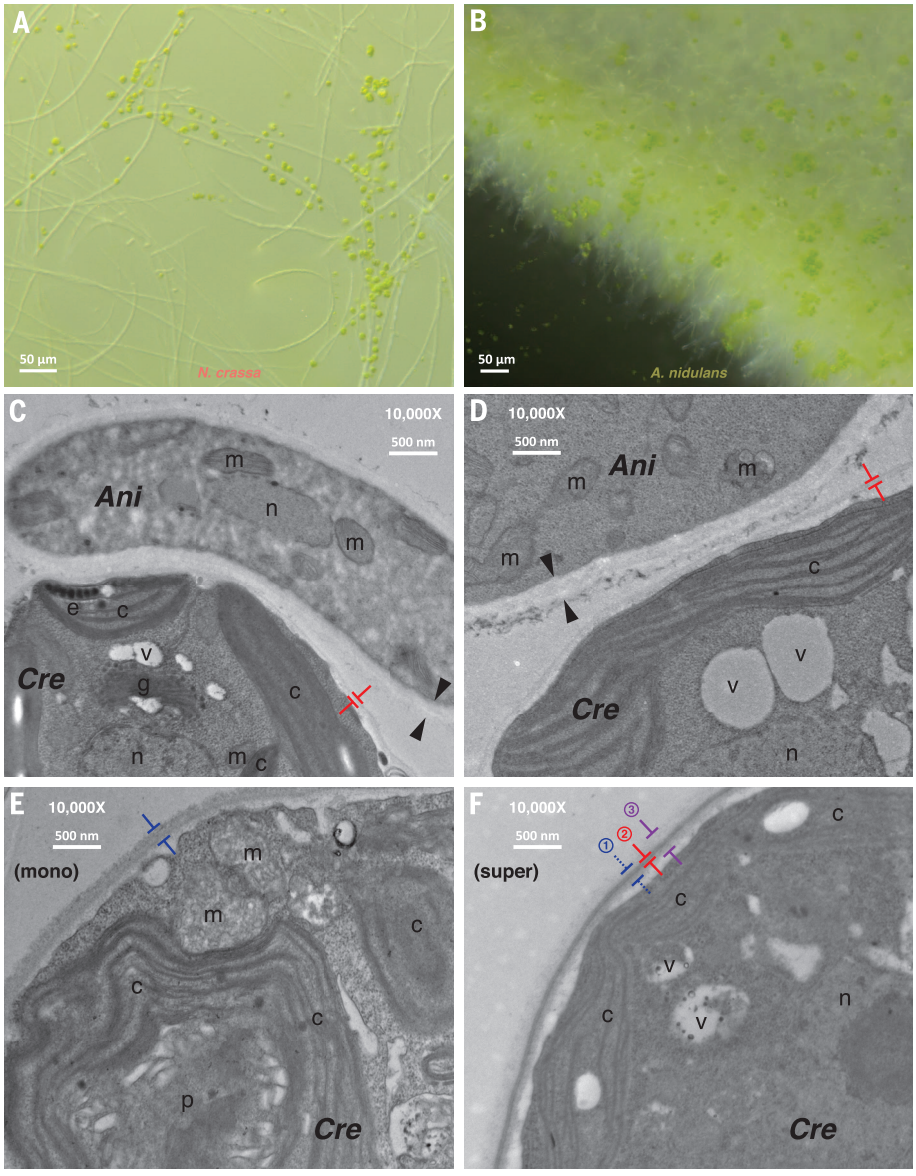

Fig. 4. *C. reinhardtii* physically associates with *N. crassa* and *A. nidulans*. Representative light micrographs of the periphery of fungal-algal associations formed in obligate mutualistic coculture. *C. reinhardtii* cells (green) stick to hyphae (white filaments) of (**A**) *N. crassa* (FGSC 11007 Δ*nit-4*) or (**B**) *A. nidulans* (TS003 *crnA- crnB-*). (**C** to **F**) Representative transmission electron micrographs reveal a simple wall-to-wall interface between *C. reinhardtii* (*Cre*) cells and *A. nidulans* (*Ani*) hyphae. Opposed arrows indicate the thickness of fungal cell walls, and opposed colored T-bars indicate those of algal cells [(C): 51 ± 10 nm; (D): 60 ± 7 nm; mean ± SD]. (E) *C. reinhardtii* grown in monoculture (160 ± 20 nm; blue T-bars) or (F) unattached *C. reinhardtii* isolated from the supernatant of the same coculture {T-demarcations: reference monoculture cell wall thickness [blue dashed; see (E)]; (2) core (heavy) cell wall staining (red): 50 ± 4 nm; (3) diffuse cell wall staining (purple): 260 ± 30 nm)} (*15*). Labeled intracellular components: c, chloroplast; e, eyespot; g, Golgi; m, mitochondria; n, nucleus; p, pyrenoid; and v, vacuole.

REFERENCES AND NOTES

1. J. N. Thompson, *Science* **284**, 2116–2118 (1999).
2. J. L. Bronstein, in *The Princeton Guide to Ecology*, S. A. Levin *et al.*, Eds. (Princeton Univ. Press, Princeton, NJ, 2009), pp. 233–238.
3. R. M. Brucker, S. R. Bordenstein, *Trends Ecol. Evol.* **27**, 443–451 (2012).
4. S. Paracer, V. Ahmadjian, *Symbiosis: An Introduction to Biological Associations* (Oxford Univ. Press, New York, 2000).
5. A. E. Douglas, *The Symbiotic Habit* (Princeton Univ. Press, Princeton, NJ, 2010).
6. J. L. Sachs, R. G. Skophammer, J. U. Regus, *Proc. Natl. Acad. Sci. U.S.A.* **108** (suppl. 2), 10800–10807 (2011).
7. J. J. Morris, R. E. Lenski, E. R. Zinser, *MBio* **3**, e00036-e12 (2012).
8. D. H. Janzen, *Oikos* **45**, 308–310 (1985).
9. S. J. Agosta, J. A. Klemens, *Ecol. Lett.* **11**, 1123–1134 (2008).
10. F. Lutzoni, M. Pagel, V. Reeb, *Nature* **411**, 937–940 (2001).
11. R. Honegger, in *Fungal Associations*, B. Hock, Eds. (Springer, Berlin, 2012), pp. 287–339.
12. D. L. Hawksworth, *Bot. J. Linn. Soc.* **96**, 3–20 (1988).
13. J. Kohlmeyer, E. J. A. Kohlmeyer, in *Marine Mycology: The Higher Fungi* (Academic Press, New York, 1979), pp. 70–78.
14. M. P. Azuara, P. J. Aparicio, *Plant Physiol.* **71**, 286–290 (1983).
15. Materials and methods are available as supplementary materials on *Science* Online.
16. M. J. I. Müller, B. I. Neugeboren, D. R. Nelson, A. W. Murray, *Proc. Natl. Acad. Sci. U.S.A.* **111**, 1037–1042 (2014).
17. J. N. Holland, D. L. DeAngelis, *Ecology* **91**, 1286–1295 (2010).
18. J. C. Slot, D. S. Hibbett, *PLOS ONE* **2**, e1097 (2007).

19. M. J. Wade, *Nat. Rev. Genet.* **8**, 185–195 (2007).
20. R. Honegger, *New Phytol.* **103**, 785–795 (1986).
21. J. M. Gómez, M. Verdú, F. Perfectti, *Nature* **465**, 918–921 (2010).
22. W. Harcombe, *Evolution* **64**, 2166–2172 (2010).
23. K. L. Hillesland, D. A. Stahl, *Proc. Natl. Acad. Sci. U.S.A.* **107**, 2124–2129 (2010).
24. N. Klitgord, D. Segrè, *PLOS Comput. Biol.* **6**, e1001002 (2010).
25. B. Momeni, C. C. Chen, K. L. Hillesland, A. Waite, W. Shou, *Cell. Mol. Life Sci.* **68**, 1353–1368 (2011).

ACKNOWLEDGMENTS

We thank Q. Justman, B. Stern, A. Pringle, S. Sasso, M. Dayel, N. Collins, J. Hess, M. Mueller, G. Frenkel, S. Kryazhimskiy, M. McDonald, D. Van Dyken, E. Wallace, K. Zimmerman, P. Boynton, J. Calarco, D. Chiang, Y. Eun, K. Foster, R. Losick, W. Tong, Y. Katz, and members of the Murray and Nelson labs for helpful feedback. We thank D. Thompson, M. Dunham, F. Winston, and N. Rhind for yeast strains; T. Schinko and J. Strauss for *A. nidulans* strains; and the Fungal Genetics Stock Center (Kansas City, MO) for fungal strains. We thank P. Rogers, M. Tam, and B. Tilton (Faculty of Arts and Sciences Center for Systems Biology FACS Core); B. Goetze, C. Kraft, and D. Richardson (Harvard Center for Biological Imaging); M. Yankova and S. King (Central Electron Microscopy Facility, University of Connecticut Health Center) for their resources and assistance; and U. Goodenough for her help in interpreting electron micrographs. Supported in part by a Jane Coffin Childs postdoctoral fellowship to E.F.Y.H. and by the National Institute of General Medical Sciences Center for Modular Biology (NIH grant P50-GM068763). Additional data described in this work can be found in the online supplementary materials. E.F.Y.H. conceived the project, performed the experiments, and analyzed the data. E.F.Y.H. and A.W.M. devised the research and wrote the manuscript. A.W.M. supported and provided input throughout all stages of this work.

SUPPLEMENTARY MATERIALS

www.sciencemag.org/content/345/6192/94/suppl/DC1
Materials and Methods
Figs. S1 to S7
Tables S1 to S8
Movies S1 to S16
References (*26*–*71*)

13 March 2014; accepted 22 May 2014
10.1126/science.1253320

CELL DEATH

Opposing unfolded-protein-response signals converge on death receptor 5 to control apoptosis

Min Lu,[1*] David A. Lawrence,[1*] Scot Marsters,[1] Diego Acosta-Alvear,[2,3] Philipp Kimmig,[2,3] Aaron S. Mendez,[2,3] Adrienne W. Paton,[4] James C. Paton,[4] Peter Walter,[2,3]† Avi Ashkenazi[1]†

Protein folding by the endoplasmic reticulum (ER) is physiologically critical; its disruption causes ER stress and augments disease. ER stress activates the unfolded protein response (UPR) to restore homeostasis. If stress persists, the UPR induces apoptotic cell death, but the mechanisms remain elusive. Here, we report that unmitigated ER stress promoted apoptosis through cell-autonomous, UPR-controlled activation of death receptor 5 (DR5). ER stressors induced *DR5* transcription via the UPR mediator CHOP; however, the UPR sensor IRE1α transiently catalyzed *DR5* mRNA decay, which allowed time for adaptation. Persistent ER stress built up intracellular DR5 protein, driving ligand-independent DR5 activation and apoptosis engagement via caspase-8. Thus, DR5 integrates opposing UPR signals to couple ER stress and apoptotic cell fate.

The endoplasmic reticulum (ER) mediates folding and maturation of transmembrane and secreted proteins (*1*, *2*). Elevated physiological demand for protein folding can cause misfolded proteins to accumulate in the ER lumen—a condition called ER stress. The unfolded protein response (UPR) senses such stress and mediates cellular adaptation by expanding the ER's protein-folding capacity while decreasing its synthetic load. Protein kinase R (PKR)–like kinase (PERK) and inositol-requiring enzyme 1α (IRE1α) are two key metazoan UPR sensors (*1*, *2*); residing in the ER membrane, each has a lumenal domain that detects misfolded polypeptides. PERK harbors a cytoplasmic kinase moiety that phosphorylates eukaryotic translation-initiation factor 2α (eIF2α). This suppresses general translation but promotes synthesis of preferred factors—including ATF4, which activates the UPR transcription factor CCAAT/enhancer-binding protein homologous protein (CHOP), among other genes. IRE1α has both kinase and endoribonuclease (RNase) cytoplasmic moieties (*3*). The kinase controls RNase activity, which mediates regulated IRE1α-dependent decay (RIDD) of ER-associated mRNAs (*4*) and generates the UPR transcription factor X-box binding protein 1 spliced (XBP1s). Certain pathological conditions can cause irresolvable ER stress (*5*), often leading to apoptotic cell death (*1*, *2*, *6*). Two interconnected signaling cascades control apoptosis: the intrinsic, mitochondrial pathway, and the extrinsic, death-receptor pathway (*7*). Each engages distinct proteases, called initiator caspases, to activate a common set of executioner caspases (*8*). Unmitigated ER stress regulates the intrinsic pathway via several Bcl-2 family proteins (*1*, *2*, *6*, *9*, *10*). Furthermore, IRE1α cleaves specific micro-RNAs to derepress caspase-2 expression (*11*); however, caspase-2 may be dispensable for ER stress-induced apoptosis (*12*), which leaves the underlying initiation mechanisms obscure.

[1]Cancer Immunology, Genentech, Inc., 1 DNA Way, South San Francisco, CA 94080, USA. [2]Howard Hughes Medical Institute, University of California, San Francisco, CA 94158, USA. [3]Department of Biochemistry and Biophysics, University of California, San Francisco, CA 94158, USA. [4]Research Centre for Infectious Diseases, School of Molecular and Biomedical Science, University of Adelaide, South Australia, 5005, Australia.
*These authors contributed equally to this work. †**Corresponding author. E-mail: peter@walterlab.ucsf.edu (P.W.); aa@gene.com (A.A.)**

Experiments with biological and pharmacological ER stressors revealed consistent activation of caspase-8, the pivotal initiator in the extrinsic pathway (*8*) (Fig. 1). The bacterial AB5 subtilase cytotoxin SubAB induces pathophysiological ER stress by cleaving the chaperone BiP (*13*). SubAB caused dose-dependent BiP depletion and ER stress, evident by CHOP and XBP1s up-regulation, in KMS11 multiple myeloma cells (Fig. 1A). In keeping with data that PERK activity persists, whereas IRE1α activation is transient (*14*), CHOP remained elevated, whereas XBP1s declined by 24 hours. SubAB also induced activation of caspase-8 and caspase-3 by 24 hours, evident by cleaved caspase and poly(ADP ribose) polymerase (PARP) products. SubAB substantially increased caspase-8 and caspase-3/7 enzymatic activity, and DNA fragmentation—an apoptotic hallmark (fig. S1, A to C). Brefeldin-A (BfA)—an inhibitor of ER-to-Golgi trafficking—similarly induced ER stress, caspase activation, and apoptosis in SK-MES-1 lung carcinoma cells (Fig. 1B and fig. S1, D to F). The sarcoplasmic ER calcium–adenosine triphosphatase inhibitor thapsigargin (Tg) induced persistent CHOP and transient XBP1s expression in wild-type and in *Bax*$^{-/-}$ HCT116 colon carcinoma cells; whereas apoptosis required *Bax*, caspase-8 activation did not (Fig. 1, C and D, and fig. S1, G to I). Moreover, small interfering RNA (siRNA) depletion of caspase-8, but not caspase-2, blocked activation of caspase-3/7 and apoptosis by diverse ER stressors (Fig. 1, E and F, and fig. S1, J to O). Caspase-8 activates the Bcl-2 family protein Bid to engage the intrinsic pathway via Bax (*15*, *16*). Full-length Bid declined in association with Tg-induced caspase-8 activation (fig. S1I), which indicated Bid processing. Bid siRNA knockdown commensurately attenuated Tg-induced apoptosis, whereas caspase-8 siRNA inhibited both Bid processing and apoptosis (fig. S1, P to S). Tg also up-regulated Bim (fig. S1I) as reported (*10*); however, caspase-8 and Bid processing occurred much earlier, which suggests that Bim might support later apoptotic signals. Thus, caspase-8 plays a pivotal role, whereas caspase-2 appears dispensable, during apoptosis induction by unmitigated ER stress.

Upon binding of cognate extracellular ligands, the death receptors Fas, DR4, or DR5 nucleate a death-inducing signaling complex (DISC) at the plasma membrane, which activates caspase-8 via